

Carbon Dioxide Transfer with Chemical Equilibrium Reactions: An Alternative Mathematical Approach

A. Shanableh

Department of Civil and Environmental Engineering,
University of Sharjah, P.O. Box 27272, Sharjah, United Arab Emirates

Abstract: Problem statement: Despite intensive research efforts on CO₂ transfer, mathematical models that describe the dependence of the CO₂ transfer rate on the pH and the degree of rate enhancement due to CO₂ chemical reactions remain unavailable. **Approach:** Such models are essential for assessing and accurately describing the progress of the CO₂ transfer process. **Results:** In this study, an alternative view of CO₂ transfer with chemical reactions was used to develop simple mathematical models to describe the pH dependence and degree of enhancement of the CO₂ transfer rate. In the alternative view, the driving force for CO₂ transfer was described in terms of the differences in the concentrations of the various carbonic species in the bulk liquid (i.e., $\Delta C_{\Delta(H_2CO_3^*)}$, $\Delta C_{\Delta(HCO_3^-)}$ and $\Delta C_{\Delta(CO_3^{2-})}$) in time (i.e., between time, t, and the time when equilibrium is achieved, t_{Eq}) rather than in terms of the concentrations gradients across the liquid film. Using the concentration differences in time, simple mathematical models describing the pH dependence of the CO₂ transfer rate and the contributions of the various carbonic species to the rate were formulated. Furthermore, the degree of CO₂ transfer rate enhancement due to CO₂ reactions in water was considered proportional to the sum of the rates of HCO₃⁻ and CO₃²⁻ transfer. **Conclusion/Recommendations:** The mathematical models were tested using data from batch and continuous-flow CO₂ transfer experiments, and the results revealed that the mathematical models explained the experimental data in an excellent manner.

Key words: CO₂ transfer, transfer rate, mathematical models, pH-dependant transfer rate, contributions of carbonic species to the transfer rate, enhancement of CO₂ transfer

INTRODUCTION

Carbon dioxide exchange across the gas/liquid interface is related to numerous natural and engineered processes and as such, the topic is of multidisciplinary interest in the scientific community^[1-6]. The theory and mathematics describing CO₂ transfer have generally evolved in agreement with earlier concepts describing the process in natural and engineered systems^[7-10]. The current CO₂ transfer theory relies on steady-state chemical equilibrium models to describe the impact of CO₂ transfer on the pH of aqueous solutions. However, the dependence of the CO₂ transfer rate on the pH and the variations of pH during CO₂ transfer are typically ignored. Furthermore, there are no mathematical models that explicitly and accurately describe the dependence of the CO₂ transfer rate on the pH. Similarly, there are no mathematical models to describe the degree of enhancement of the CO₂ transfer rate as a function of pH due to chemical reactions involving hydration (de-hydration) of CO₂ and acid-base ionization reactions leading to the formation (or

removal) of HCO₃⁻ and CO₃²⁻. As such, the main objective of the study was to develop simple mathematical models to describe the dependence of the CO₂ transfer rate on the pH and the degree of rate enhancement due to chemical reactions.

In the current theory, the CO₂ transfer rate is mathematically described through comparing the relative rates of CO₂ diffusion and chemical reactions across the Liquid Layer (LL) with thickness equal to δ_{LL} , with the rate of CO₂ transfer being controlled by the slower of the two processes. For example, Emerson^[8] and Stumm and Morgan^[10] described the concentration gradient (ΔC) across the liquid layer that drives CO₂ flux ($F = \frac{D}{\delta_{LL}} \Delta C$, where D is the diffusion coefficient) based on which of the two processes is faster, as follows:

- In the case where diffusion of CO₂ through the liquid layer is slow compared to the rates of reactions (i.e., diffusion controlled transfer), then

HCO_3^- and CO_3^{2-} form within the liquid layer and thus concentration gradients develop for each of the carbonic species within the layer. In this case, ΔC is that for total carbonic species with the contributions of HCO_3^- and CO_3^{2-} enhancing the overall CO_2 transfer rate, as in Eq. 1:

$$F = F_{\text{CO}_2} + F_{\text{HCO}_3^-} + F_{\text{CO}_3^{2-}} \quad (1)$$

- In the case where CO_2 diffusion through the liquid film is fast compared to the rates of chemical reactions (i.e., chemically controlled transfer), then HCO_3^- and CO_3^{2-} are not formed or consumed within the diffusion zone due to chemical reactions and the diffusion of CO_2 alone accounts for transport with the concentration gradient, ΔC , being that in CO_2 alone

In the chemically controlled transfer process, equilibrium is not achieved within the LL during CO_2 transfer, but beyond in the bulk liquid. In the diffusion controlled CO_2 transfer process, chemical equilibrium may or may not develop within the LL, depending on the rates of chemical reactions compared to slow diffusion. If chemical reactions are assumed to be instantaneous, which is unlikely, then equilibrium is achieved everywhere within the LL. Stumm and Morgan^[10] and Morel and Hering^[11] suggested that enhancement of CO_2 transfer is not considered significant except in alkaline waters or very quiescent water bodies.

Livansky^[12] studied the rate of absorption of carbon dioxide as a function of pH in different buffers and concluded that the absorption rate increased for all buffers tested with increasing pH. Howe and Lawler^[13] presented a mathematical model, Eq. 2, to describe the relationship between the CO_2 transfer rate and pH over a wide range of pH, as in Eq. 2:

$$r_c = \alpha_g K_L a (C_{T,Eq} - C_T) \quad (2)$$

Where:

C_T = The concentration of total carbonic species in the bulk liquid

$C_{T,Eq}$ = The equilibrium concentration in the bulk liquid as determined by Henry's law

α_g = $[\text{H}_2\text{CO}_3^*]/[C_T]$, which is pH dependent

$K_L a$ = Mass transfer coefficient

Howe and Lawler^[13] described the model in Eq. 2 as being suitable for use whether the pH changes or not as a result of pH transfer. However, due to the change in pH as a result of CO_2 transfer, the use of α_g as a

common factor that applies to both C_T and $C_{T,Eq}$ may not be appropriate. As such, the model is not suitable for use except in the special and unlikely case in which the pH does not change or is not allowed to change due to CO_2 transfer.

In this study, an alternative view of CO_2 transfer with chemical reactions was used to facilitate the development of simple mathematical models to describe the pH dependence and degree of enhancement of the CO_2 transfer rate. The alternative view was based on describing CO_2 transfer rate in terms of the ultimate driving force represented by the difference in time between the concentration of aqueous CO_2 in the bulk liquid at any time (t) and the ultimate concentration of aqueous CO_2 at the time of equilibrium (t_{Eq}). Using the mathematical description of the ultimate driving force, as described in the following sections, the degree of CO_2 transfer rate enhancement was estimated based on the contributions of the various carbonic species to the transfer rate, which were considered proportional to their concentration gradients in time. The development of the mathematical models is described in details in the following section.

Theoretical considerations: Stumm and Morgan^[10] accounted for the enhancement of the CO_2 transfer rate through expressing the concentration gradient in aqueous CO_2 alone (chemically controlled transfer without enhancement) or in the total carbonic species (diffusion controlled transfer with rate enhancement). In the case where diffusion is fast compared to chemical reactions, HCO_3^- and CO_3^{2-} are not formed (or consumed to release CO_2) nor chemical equilibrium among the carbonic species is achieved within the LL. In this case, formation (or consumption) of HCO_3^- and CO_3^{2-} and establishment of chemical equilibrium require more time than available within the LL. As such, rapid diffusion results in excess or deficiency in CO_2 concentration in the bulk liquid that is not in equilibrium with the other carbonic species but requires additional time or space to achieve equilibrium. Current theory however does not account for the extra time or space needed to achieve chemical equilibrium in the bulk liquid. In fact, chemical reactions work on bringing the carbonic species in chemical equilibrium with each other, whether such reactions take place in the traditionally defined LL or in the bulk liquid and as such the influence of chemical reactions on the transfer rate cannot be separated from the mass transfer process.

In the case where diffusion is slow compared to the rates of chemical reactions, HCO_3^- and CO_3^{2-} form

within the LL. Slow diffusion may also allow enough time for chemical equilibrium to be established within the LL. Theoretically, if the chemical reactions were considered to be instantaneous, which is unlikely, then chemical equilibrium among the carbonic species is achieved everywhere within the LL and the bulk liquid.

The target of both diffusion and chemical reactions is to achieve equilibrium between the concentrations of CO₂ in the gas and bulk liquid and also chemical equilibrium among the various carbonic species (CO₂, H₂CO₃, HCO₃⁻ and CO₃²⁻). When equilibrium is disturbed, both processes proceed to reestablish a new state of equilibrium in which net diffusion ceases when equilibrium among the carbonic species is reestablished. As such, the ultimate driving force for CO₂ transfer must be the concentration difference between two equilibrium states separated by the time required to reestablish equilibrium in terms of diffusion and chemical reactions. Using the ultimate driving force accounts for the time required to establish chemical equilibrium among the carbonic species.

Using H₂CO₃^{*} to represent aqueous CO₂, which includes both dissolved CO₂ and H₂CO₃, the ultimate driving force can be mathematically described as the difference in time between the concentration of H₂CO₃^{*} in the bulk liquid at any time, or [H₂CO₃^{*}]_(t) and the ultimate concentration of H₂CO₃^{*} at the time of equilibrium, or [H₂CO₃^{*}]_(t_{Eq}). Mathematically, the ultimate driving force can be described as ΔC_{Δt} = [H₂CO₃^{*}]_(t_{Eq}) - [H₂CO₃^{*}]_(t). The current CO₂ transfer theory is based on describing the driving force using the concentration gradient in space (i.e., across the liquid layer with thickness equal to δ_{LL}). The ultimate concentration difference in time (ΔC_{Δt} = [H₂CO₃^{*}]_(t_{Eq}) - [H₂CO₃^{*}]_(t)) can be considered equivalent to the ultimate concentration gradient in space across the liquid layer, or ΔC_{Δx(t)} = [H₂CO₃^{*}]_{x=0} - [H₂CO₃^{*}]_{x=δ_{LL}}. The equivalency between the concentration difference in time and space assumes that [H₂CO₃^{*}]_{x=0} = [H₂CO₃^{*}]_(t_{Eq}) and [H₂CO₃^{*}]_{x=δ_{LL}} = [H₂CO₃^{*}]_(t). A view of the ultimate concentration difference in time and space is presented in Fig. 1. The equivalency between the driving force in time and space provides important insight into the progress of diffusion and reaction across the LL. For example, the equivalent concentration profiles for the various carbonic species and the pH across the LL at any time can be considered equivalent to the variations of the carbonic

species concentrations and the pH with time leading to equilibrium as described by Henry's law.

Mathematical considerations: According to the two films gas transfer theory, CO₂ flux in the liquid and gas films is driven by the corresponding concentration gradients, as expressed in Eq. 3 and 4:

$$F_{LL} = K_L (H_2CO_{3Int}^* - H_2CO_{3(t)}^*) \quad (3)$$

$$F_{GL} = K_g (CO_{2G} - CO_{2G.Int}) \quad (4)$$

Where:

- F_{LL} = Flux across the liquid layer
- F_{GL} = Flux across the gas layer
- H₂CO_{3Int}^{*} = Concentration of aqueous CO₂ in the liquid at the gas/liquid interface
- H₂CO_{3(t)}^{*} = Concentration of aqueous CO₂ in the bulk liquid at time t
- CO_{2G.Int} = Concentration of gaseous CO₂ in the gas phase at the interface
- CO_{2G} = Concentration of gaseous CO₂ in the bulk gas phase
- K_L and K_g = Liquid and gas phase transfer coefficients, respectively

Equating flux across the liquid film with flux across the gas film (Eq. 5), then substituting for CO_{2G.Int} and CO_{2G} from Henry's law (Eq. 6 and 7) into Eq. 5 and solving for CO_{2Int} results in Eq. 8. Substituting from Eq. 8 into Eq. 3 results in Eq. 9-11:

$$K_L (H_2CO_{3Int}^* - H_2CO_{3(t)}^*) = K_g (CO_{2G} - CO_{2G.Int}) \quad (5)$$

$$CO_{2G} = H_n H_2CO_{3(tEq)}^* \quad (6)$$

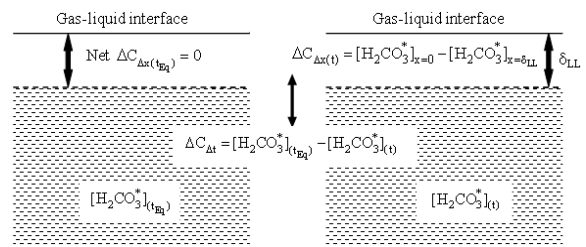


Fig. 1: A simplified view of CO₂ transfer with the concentration gradient across the LL (i.e., gradient in space) is equivalent to the concentration difference in the bulk liquid in time (i.e., between any time during CO₂ transfer and the time when equilibrium as defined by Henry's law is achieved)

$$CO_{2G,Int} = H_n H_2CO_{3Int} \quad (7)$$

$$H_2CO_{3Int} = \frac{K_1 H_2CO_{3(t)} + H_n K_g H_2CO_{3(t_{Eq})}^*}{K_1 + H_n K_g} \quad (8)$$

$$F_{LL} = \frac{H_n K_g K_1}{K_1 + H_n K_g} (H_2CO_{3(t_{Eq})}^* - H_2CO_{3(t)}^*) \quad (9)$$

$$F_{LL} = K_L (H_2CO_{3(t_{Eq})}^* - H_2CO_{3(t)}^*) \quad (10)$$

$$K_L = \frac{H_n K_g K_1}{K_1 + H_n K_g} \quad (11)$$

Where:

$H_2CO_{3(t_{Eq})}^*$ = Concentration of aqueous CO_2 in the bulk liquid at the time when equilibrium according to Henry's law is achieved

H_n = Henry's law constant

The gas transfer rate (r_c) can be obtained by multiplying the flux in Eq. 10 by the specific surface area (a) of contact between the gas and liquid phases at the interface, as in Eq. 12:

$$r_c = K_L a (H_2CO_{3(t_{Eq})}^* - H_2CO_{3(t)}^*) \quad (12)$$

Using molar concentrations, the transfer rate can be expressed as in Eq. 13:

$$r_c = K_L a \left([H_2CO_3^*]_{(t_{Eq})} - [H_2CO_3^*]_{(t)} \right) \quad (13)$$

Noting that the pH in the bulk liquid changes as a result of mass transfer from $pH_{(t)}$ to $pH_{(t_{Eq})}$ and with chemical equilibrium established among the carbonic species in the bulk liquid, the transfer rate in Eq. 13 can be expressed in terms of the total and other carbonic species according to their relative abundance, as follows:

$$r_c = K_L a \left(\alpha_{o(t_{Eq})} [TC]_{(t_{Eq})} - \alpha_{o(t)} [TC]_{(t)} \right) \quad (14)$$

$$r_c = K_L a \left(\frac{\alpha_{o(t_{Eq})} [HCO_3^-]_{(t_{Eq})}}{\alpha_{1(t_{Eq})}} - \frac{\alpha_{o(t)} [HCO_3^-]_{(t)}}{\alpha_{1(t)}} \right) \quad (15)$$

$$r_c = K_L a \left(\frac{\alpha_{o(t_{Eq})} [CO_3^{2-}]_{(t_{Eq})}}{\alpha_{2(t_{Eq})}} - \frac{\alpha_{o(t)} [CO_3^{2-}]_{(t)}}{\alpha_{2(t)}} \right) \quad (16)$$

Where:

$[TC]_{(t)}$ = The concentration of total carbonic species in the bulk liquid at any time

$[TC]_{(t_{Eq})}$ = The equilibrium concentration in the bulk liquid as determined by Henry's law

α = The different (α) values represent the relative abundance of the carbonate species in solution as defined in Table 1, with $[H^+][HCO_3^-]/[H_2CO_3^*] = k_1$ and $[H^+][CO_3^{2-}]/[HCO_3^-] = k_2$

Practical considerations: In practical CO_2 absorption and desorption applications, the CO_2 transfer rate is assessed through measuring the concentration of the total carbonic species TC in the aqueous phase or the concentration of CO_2 in the gas phase, or both. In such applications, it is convenient to express the transfer rate using the concentration of the total carbonic species, as presented in Eq. 17, below:

$$r_c = K_L a_{(Apparent)} \left([TC]_{(t_{Eq})} - [TC]_{(t)} \right) \quad (17)$$

where, $K_L a_{(Apparent)}$ is apparent mass transfer coefficient.

By comparing Eq. 14 and 17, the relationship between $K_L a_{(Apparent)}$ and $K_L a$ can be expressed as in Eq. 18:

$$\frac{K_L a_{(Apparent)}}{K_L a} = \frac{\alpha_{o(t_{Eq})} [TC]_{(t_{Eq})} - \alpha_{oAq} [TC]_{(t)}}{[TC]_{(t_{Eq})} - [TC]_{(t)}} \quad (18)$$

Transfer rate enhancement due to chemical reactions: Equation 14 and 17, expressed in terms of the concentration gradient in total carbonic species account for enhanced CO_2 transfer, with its various components, as follows:

$$r_c = r_{H_2CO_3^*} + r_{HCO_3^-} + r_{CO_3^{2-}} \quad (19)$$

As such, the contributions of the various carbonic species to the overall transfer rate can be expressed in terms of their relative abundance as follows:

$$r_{H_2CO_3^*} = K_L a \left(\alpha_{o(t_{Eq})} \alpha_{o(t_{Eq})} [TC]_{(t_{Eq})} - \alpha_{o(t)} \alpha_{o(t)} [TC]_{(t)} \right) \quad (20)$$

$$r_{HCO_3^-} = K_L a \left(\alpha_{1(t_{Eq})} \alpha_{o(t_{Eq})} [TC]_{(t_{Eq})} - \alpha_{1(t)} \alpha_{o(t)} [TC]_{(t)} \right) \quad (21)$$

$$r_{CO_3^{2-}} = K_L a \left(\alpha_{2(t_{Eq})} \alpha_{o(t_{Eq})} [TC]_{(t_{Eq})} - \alpha_{2(t)} \alpha_{o(t)} [TC]_{(t)} \right) \quad (22)$$

Table 1: Relative abundance of carbonic species at any time and at the time when equilibrium according to Henry's law is achieved

Values at pH _(t)	Values at pH _(t_{Eq})
$\alpha_{o(t)} = \frac{[H_2CO_3^*]_{(t)}}{[TC]_{(t)}} = \left(1 + \frac{k_1}{[H^+]_{(t)}} + \frac{k_1 k_2}{[H^+]_{(t)}^2} \right)^{-1}$	$\alpha_{o(t_{Eq})} = \frac{[H_2CO_3^*]_{(t_{Eq})}}{[TC]_{(t_{Eq})}} = \left(1 + \frac{k_1}{[H^+]_{(t_{Eq})}} + \frac{k_1 k_2}{[H^+]_{(t_{Eq})}^2} \right)^{-1}$
$\alpha_{1(t)} = \frac{[HCO_3^-]_{(t)}}{[TC]_{(t)}} = \left(1 + \frac{[H^+]_{(t)}}{k_1} + \frac{k_2}{[H^+]_{(t)}} \right)^{-1}$	$\alpha_{1(t_{Eq})} = \frac{[HCO_3^-]_{(t_{Eq})}}{[TC]_{(t_{Eq})}} = \left(1 + \frac{[H^+]_{(t_{Eq})}}{k_1} + \frac{k_2}{[H^+]_{(t_{Eq})}} \right)^{-1}$
$\alpha_{2(t)} = \frac{[CO_3^{2-}]_{(t)}}{[TC]_{(t)}} = \left(1 + \frac{[H^+]_{(t)}}{k_2} + \frac{[H^+]_{(t)}^2}{k_1 k_2} \right)^{-1}$	$\alpha_{2(t_{Eq})} = \frac{[CO_3^{2-}]_{(t_{Eq})}}{[TC]_{(t_{Eq})}} = \left(1 + \frac{[H^+]_{(t_{Eq})}}{k_2} + \frac{[H^+]_{(t_{Eq})}^2}{k_1 k_2} \right)^{-1}$

Based on the above equations, CO₂ transfer without enhancement can be represented by r_{H₂CO₂}, as expressed in Eq. 20. The Enhancement Factor (EF) thus can be defined as in Eq. 23, below:

$$EF(\%) = \frac{r_{HCO_3^-} + r_{CO_3^{2-}}}{r_C} \times 100 \quad (23)$$

MATERIALS AND METHODS

Experimental evaluation: Because the behavior of CO₂ absorption and desorption is well known and predictable, a detailed CO₂ experimental program was not deemed necessary. Instead, available experimental data, conducted under the conditions described below, were used to clarify various aspects and applications of the theory.

Two sets of batch experiments were conducted at different initial pH values in a 15 cm diameter × 40 cm height cylinder filled with five liters carbonate solution. In the first set, a phosphate buffer (0.05 M) was added to reduce pH increase due to CO₂ removal. In the second set, no phosphate buffer was added. The initial total inorganic carbon in each solution was designed to be approximately 100 mg L⁻¹. During each experiment, Helium was bubbled at the bottom of the cylinder for 30 min and the total inorganic carbon concentration and pH were measured with time.

The continuous-flow, packed column experiments were conducted in a 15 cm diameter × 100 cm height cylinder (Fig. 2) filled with plastic media to a depth of 82 cm. The experiments were conducted using a solution containing 0.05 M phosphate pumped separately from the solution containing the inorganic carbonates. The liquid stream was introduced at the top of the column. Air was introduced at the bottom of the column. The experiments were conducted at different initial pH values and the pH and inorganic carbon concentration in samples collected from the column influent and effluent were measured over a period of time until steady-state removal results were attained.

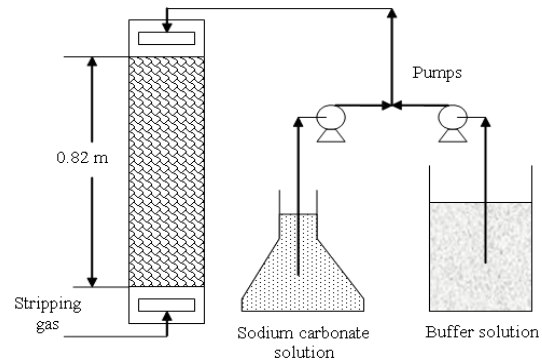


Fig. 2: Schematic of the continuous-flow counter-current CO₂ desorption column

RESULTS

With the desorption gas CO₂-free and with [TC]_(t_{Eq}) = 0, the general transfer rate presented in Eq. 17 reduces to the form expressed in Eq. 24. Assuming that the pH remains unchanged in the PO₄ buffered solution, then K_La_(Apparent) remains constant and the integrated form of Eq. 24 is expressed in Eq. 25:

$$\frac{d[TC]_{(t)}}{dt} = -K_{L}a_{(Apparent)}[TC]_{(t)} = -\alpha_{o(t)} K_{L}a [TC]_{(t)} \quad (24)$$

$$\ln[TC]_t = \ln[TC]_{t=0} - K_{L}a_{(Apparent)}t \quad (25)$$

Based on Eq. 25, the K_La_(Apparent) values were determined from the slopes of the lines of best-fit expressing the linear relationships between ln[TC]_t versus time for each of the desorption experiments conducted at different initial pH values. The relationship between the resulting K_La_(Apparent) values and removals achieved are presented in Fig. 3. The results matched the expected relationship between K_La_(Apparent) and K_La as predicted from Eq. 18 and expressed in Eq. 26:

$$K_{L}a_{(Apparent)} = \alpha_{oAq} K_{L}a \quad (26)$$

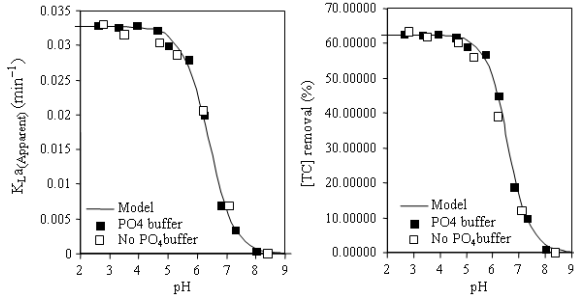


Fig. 3: Dependence of the mass transfer coefficient ($K_L a_{(Apparent)}$) and [TC] removal on the pH in the batch experiments

The theoretical pH change due to CO_2 desorption can be estimated using the alkalinity Eq. 27. Equation 27 is expressed in terms of the relevant abundance of the negatively charged carbonate species (i.e., using $\alpha_{1(t)}$ and $\alpha_{2(t)}$) and the negatively charged phosphates species (i.e., using $\alpha_{1P(t)} = [H_2PO_4^-]_{(t)}/[TP]$, $\alpha_{2P(t)} = [HPO_4^{2-}]_{(t)}/[TP]$ and $\alpha_{3P(t)} = [PO_4^{3-}]_{(t)}/[TP]$, with [TP] being the total phosphates concentration). In Eq. 27, the $Alk_{Initial}$ and [TP] do not change due to CO_2 desorption but the pH does. In this case, the pH change due to CO_2 removal reached a maximum of approximately 0.3 units:

$$Alk_{Initial} = \frac{k_w}{[H^+]_{(t)}} + (\alpha_{1(t)} + 2\alpha_{2(t)})[TC]_{(t)} + (\alpha_{1P(t)} + 2\alpha_{2P(t)} + 3\alpha_{3P(t)})[TP] - [H^+]_{(t)} \quad (27)$$

Without the phosphate buffer, the pH was allowed to increase more freely as a result of CO_2 removal using the batch system. In this case, both $K_L a_{(Apparent)}$ and $[TC]_{(t)}$ in Eq. 24 change with time as CO_2 is removed, but the initial alkalinity (Eq. 28) does not change. Solving Eq. 28 for $[TC]_{(t)}$ then substituting into Eq. 24 results in the CO_2 removal rate (Eq. 29). Using numerical integration, the model parameters (i.e., $K_L a_{(Apparent)}$ and final $pH_{(t)}$) were determined and compared with the measured values, as shown in Fig. 3. The pH change due to CO_2 desorption reached approximately 0.45 units:

$$Alk_{Initial} = \frac{k_w}{[H^+]_{(t)}} + (\alpha_{1(t)} + 2\alpha_{2(t)})[TC]_{(t)} - [H^+]_{(t)} \quad (28)$$

$$\frac{d[TC]_{(t)}}{dt} = -K_L a_{(Apparent)} \left(\frac{[H^+]_{(t)} Alk_{Initial} - k_w + [H^+]_{(t)}^2}{[H^+]_{(t)} (\alpha_{1(t)} + 2\alpha_{2(t)})} \right) \quad (29)$$

The CO_2 removal results obtained using the continuous flow system exhibited the same trends as the results obtained using the batch system. The CO_2 reaction rate equation that describes the removal of CO_2 from any section of the counter-current desorption column is expressed in Eq. 31, with:

$$dt = Adh/Q_L \quad (30)$$

Where:

A = Column cross sectional area

Q_L = Volumetric liquid flow rate

dh = Section thickness along the column height:

$$-\frac{A K_L a}{Q_L} dh = \frac{d[TC]_{(t,h)}}{(\alpha_{o(t_{Eq,h})}[TC]_{(t_{Eq,h})} - \alpha_{o(t,h)}[TC]_{(t,h)})} \quad (31)$$

A steady-state, the concentrations in the liquid and gas phases do not vary with time at any point along the column but with height. As such, Eq. 31 becomes:

$$-\frac{A K_L a}{Q_L} dh = \frac{d[TC]_{(h)}}{(\alpha_{o(t_{Eq,h})}[TC]_{(t_{Eq,h})} - \alpha_{o(h)}[TC]_{(h)})} \quad (32)$$

As the concentration of CO_2 in the gas phase increases as the gas travels up the column, the equilibrium concentration at any height can be described using Henry's law as $CO_{2G(h)} = H\alpha_{o(t_{Eq,h})}[TC]_{(t_{Eq,h})}$. A value for $\alpha_{o(t_{Eq,h})}[TC]_{(t_{Eq,h})}$ in Eq. 32 can be determined from a mass balance on the bottom section of the column $Q_G(CO_{2G(h)} - CO_{2G(ln)}) = Q_L([TC]_{(h)} - [TC]_{Effluent})$ with $CO_{2G(h)} = H\alpha_{o(t_{Eq,h})}[TC]_{(t_{Eq,h})}$. The result is the general mass transfer rate expression, Eq. 33. Assuming that the pH does not significantly change as a result of CO_2 removal, the integrated form of Eq. 33 is presented in Eq. 34:

$$-\frac{AK_L a_{(Apparent)}}{Q_L} dh = \frac{d[TC_{Aq}]_{(t)}}{\left(\frac{1 - R\alpha_{o(h)}}{R} [TC]_{(h)} - \left(\frac{1}{R} [TC]_{Effluent} + \frac{CO_{2G(ln)}}{H_n} \right) \right)} \quad (33)$$

Where:

Q_G = Volumetric gas flow rate

$CO_{2G(ln)}$ = Initial concentration of CO_2 in the desorption gas

$CO_{2G(h)}$ = Concentration of CO_2 in the desorption gas at height h

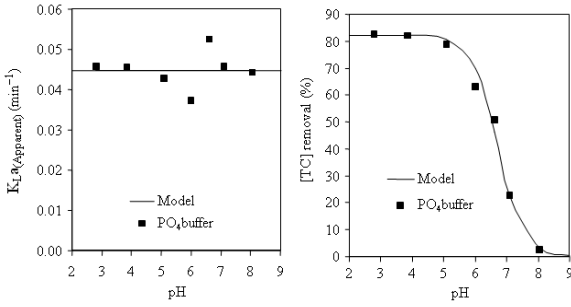


Fig. 4: Dependence of the mass transfer coefficient ($K_L a_{(Apparent)}$) and [TC] removal on the pH in the buffered column desorption experiments

[TC]_(h) = Total carbonates concentration at height h
 [TC]_{Effluent} = Total carbonates concentration in the final effluent
 $R = \frac{H_n Q_G}{Q_L}$ is the desorption factor
 h = Column height:

$$K_L a = - \frac{Q_L R}{Ah(1 - \alpha_{o(h)} R)} \ln \left[\frac{\left(\frac{1 - \alpha_{o(h)} R}{R} \right) [TC]_{(Influent)} - \left(\frac{1}{R} [TC]_{(Effluent)} - \frac{CO_{2G}(In)}{H_n} \right)}{\left(\frac{1 - \alpha_{o(h)} R}{R} \right) [TC]_{(Effluent)} - \left(\frac{1}{R} [TC]_{(Effluent)} - \frac{CO_{2G}(In)}{H_n} \right)} \right] \quad (34)$$

The data in Fig. 4 represent a direct application of Eq. 34, with the results providing good representation of the expected relationships for $K_L a$ and [TC] removals.

DISCUSSION

The enhancement of the CO₂ transfer rate due to chemical reactions is contributed by HCO₃⁻ and CO₃²⁻, with the transfer rate of H₂CO₃^{*} alone representing the case without enhancement. To illustrate the contributions of HCO₃⁻ and CO₃²⁻, the transfer rate models used in the analysis of the batch experimental results without phosphate buffer and with [TC]_(t=0) = 0 are used. For example, the contributions of the various carbonic species to the CO₂ removal rate, according to Eq. 35-37 which are based on Eq. 20-22, are depicted in Fig. 5 and 6. In Fig. 5, the contributions of the various carbonic species to the total CO₂ transfer rate and the degree of chemical enhancement, according to Eq. 23,

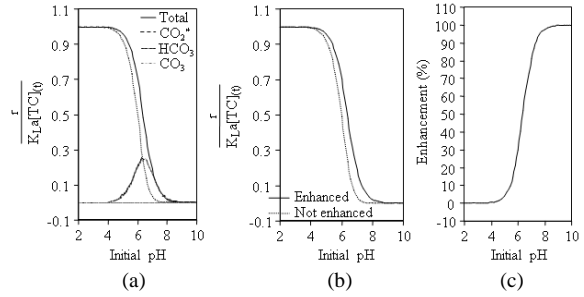


Fig. 5: Contributions of the various carbonate species to total CO₂ transfer rate (a) with comparison of the transfer rate with and without chemical enhancement (b) and degree of enhancement (c)

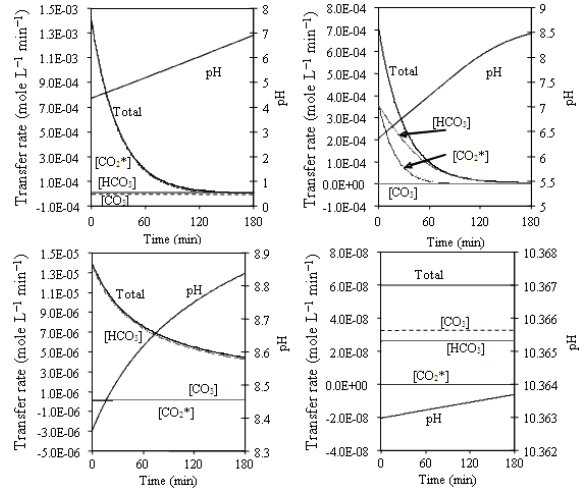


Fig. 6: Contributions of the various carbonate species to the total CO₂ transfer rate at four different initial pH values (based on the batch experimental results without the phosphate buffer)

are presented. In Fig. 6, four examples showing the variations of the contributions of the carbonic species to the transfer rate together with the increase in the pH during 180 min of CO₂ desorption at four different initial pH values are presented. The data in Fig. 5 and 6 show that the transfer rate declines as the pH increases with enhancement occurring in the range of $pk_1 - 2 < pH < pk_1 + 2$ due to the contribution of HCO₃⁻. At pH = pk_1 , the rate components contributed by H₂CO₃^{*} and HCO₃⁻ become equal, with each accounting for approximately 50 percent of the total rate. In the pH range between pk_1 and pk_2 , the rate component contributed by HCO₃⁻ has the largest value. Above pH = pk_2 , the transfer rate becomes negligible but dominated by CO₃²⁻ contribution.

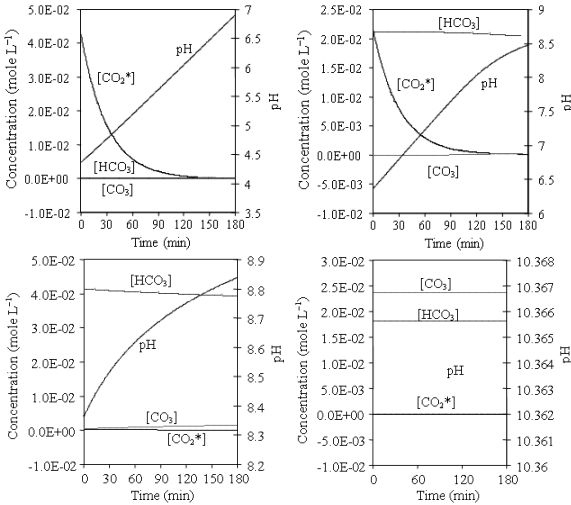


Fig. 7: Distribution of the carbonic species and the pH as time progresses during CO₂ removal (based on the batch experimental results without the phosphate buffer)

These results clearly suggest that the contributions of the various carbonic species to the transfer rate are consistent with their relative abundance in the bulk liquid.

$$r_{\text{H}_2\text{CO}_3^*} = \alpha_{o(t_{\text{Eq}})} \alpha_{o(t_{\text{Eq}})} K_L a [\text{TC}]_{(t_{\text{Eq}})} \quad (35)$$

$$r_{\text{HCO}_3^-} = \alpha_{1(t_{\text{Eq}})} \alpha_{o(t_{\text{Eq}})} K_L a [\text{TC}]_{(t_{\text{Eq}})} \quad (36)$$

$$r_{\text{CO}_3^{2-}} = \alpha_{2(t_{\text{Eq}})} \alpha_{o(t_{\text{Eq}})} K_L a [\text{TC}]_{(t_{\text{Eq}})} \quad (37)$$

The variations of the concentrations of the carbonic species and pH corresponding to the four examples presented in Fig. 6 are depicted in Fig. 7. As the transfer rate is assumed to be first order, achieving equilibrium as described by Henry's law requires infinite time. The results in Fig. 7 show 180 min of CO₂ removal, however because the transfer rate is assumed to be first order, achieving equilibrium as described by Henry's law requires infinite time. As such, the equivalence between time and space, as shown in Fig. 1, can be viewed at any time (t) as follows: $x = 0$ at $t_{\text{Eq}} = \infty$ and $x = \delta_{\text{LL}}$ at time = t. The concentration Vs time profiles shown in Fig. 7 can thus be thought of as concentration Vs distance profiles within the liquid layer at time = t.

CONCLUSION

The alternative view of CO₂ transfer with chemical reactions presented in this study was based

on describing CO₂ transfer in terms of the ultimate driving force, $\Delta C_{\Delta t} = [\text{H}_2\text{CO}_3^*]_{(t_{\text{Eq}})} - [\text{H}_2\text{CO}_3^*]_{(t)}$, or $\Delta C_{\Delta t} = \alpha_{o(t_{\text{Eq}})} [\text{TC}]_{(t_{\text{Eq}})} - \alpha_{o(t)} [\text{TC}]_{(t)}$. The use of the ultimate driving force concept allowed describing the pH dependence of the transfer rate and the degree of rate enhancement due to chemical reactions using simple and straight forward mathematical models. Furthermore, the use of the ultimate driving force allowed estimating the contribution of each of the carbonic species to the total transfer rate according to their relative abundance. The approach presented in this study simplifies the analysis of gas transfer with chemical reactions and can easily be extended to describe the transfer of other gases that undergo similar reactions leading to ultimate equilibrium in the aqueous phase.

REFERENCES

1. Cents, A.H.G., D.W.F. Brillman and G.F. Versteeg, 2001. Gas absorption in an agitated gas-liquid-liquid system. Chem. Eng. Sci., 56: 1075-1083. DOI: 10.1016/S0009-2509(00)00324-9
2. Glade, H. and A.E. Al-Rawajfeh, 2008. Modeling of CO₂ release and the carbonate system in multiple-effect distillers. Desalination, 222: 605-625. DOI: 10.1016/j.desal.2007.02.069
3. House, W.A., J.R. Howard and G. Skirrow, 1984. Kinetics of carbon dioxide transfer across the air/water interface. Faraday Discuss. Chem. Soc., 77: 33-46. DOI: 10.1039/DC9847700033
4. Sabine, C.L., R.A. Feely, N. Gruber, R.M. Key and K. Lee *et al.*, 2004. The oceanic sink for anthropogenic CO₂. Science, 305: 367-371. DOI: 10.1126/science.1097403
5. Blackford, J.C. and F.J. Gilbert, 2007. pH variability and CO₂ induced acidification in the North Sea. J. Mar. Syst., 64: 229-241. DOI: 10.1016/j.jmarsys.2006.03.016
6. Talbot, P., M.P. Gortares, R.W. Lencki and J. De la Noue, 1991. Absorption of carbon dioxide in algal mass culture systems a different characterization approach. Biotechnol. Bioeng., 37: 834-842. DOI: 10.1002/bit.260370907
7. Danckwerts, P.V., 1950. Absorption by simultaneous diffusion and chemical reaction. Trans. Faraday Soc., 46: 300-304. DOI: 10.1039/TF9504600300
8. Emerson, S., 1975. Chemically enhanced CO₂ gas exchange in a eutrophic lake: A general model. Limnol. Oceanogr., 20: 743-753. http://aslo.org/lo/toc/vol_20/issue_5/0743.pdf

9. Quinn, J.A. and N.C. Otto, 1971. Carbon dioxide exchange at the air-sea interface: Flux augmentation by chemical reaction. *J. Geophys. Res.*, 76: 1539-1549. DOI: 10.1029/JC076i006p01539
10. Stumm, W. and J.J. Morgan, 1995. *Aquatic Chemistry, Chemical Equilibria and Rates in Natural Waters*. 3rd Edn., John Wiley and Sons, Inc., New York, USA., ISBN: 0471511846, pp: 1022.
11. Morel, F.M.M. and J.G. Hering, 1993. *Principles and Applications of Aquatic Chemistry*. John Wiley and Sons, New York, USA., ISBN: 978-0-471-54896-6, pp: 608.
12. Livansky, K., 1982. Effect of temperature and pH on absorption of carbon dioxide by a free level of mixed solutions of some buffers. *Folia Microbiol.*, 27: 55-59.
<http://www.ncbi.nlm.nih.gov/pubmed/6800908>
13. Howe, K.J. and D.F. Lawler, 1989. Acid-base reactions in gas transfer: A mathematical approach. *J. Am. Water Works Assoc.*, 81: 61-66.
http://apps.awwa.org/WaterLibrary/showabstract.aspx?an=JAW_0025635